2015 IEEE International Conference on Robotics and Automation (ICRA)
Washington State Convention Center
Seattle, Washington, May 26-30, 2015

Active Sensor Networks for Nuclear Detection

Jianxin Sun, Herbert G. Tanner, and Ioannis Poulakakis

Abstract— **This paper approaches from an optimal control perspective the problem of fixed-time detection of mobile radioactive sources in transit by means of a collection of mobile sensors. Under simplifying assumptions on the geometry of the source, sensors, and surrounding environment, and with knowledge of the source's trajectory, it is shown that the optimal control problem admits an intuitive, analytic closed-form solution. This is facilitated by the availability of analytic expressions for bounds on the probabilities of detection and false alarm during a Neyman-Pearson detection test. The intuition derived from this analytic solution leads to a motion control law that steers suboptimally the sensors to an arbitrarily small neighborhood of the suspected source, while navigating among stationary obstacles in their environment, making a step closer to a practical physical implementation.**

I. Introduction

This paper derives analytic optimal motion strategies for mobile sensors aiming at detecting weak radioactive sources in transit, and then investigates provably convergent relaxations which afford implementation in constrained environments under constraints on actuation. Detecting radioactive material is relevant and timely due to the increasing risk of accidental or malicious nuclear proliferation [1], [2] and the potential demand in inspecting moving subjects without hindering traffic flow. To timely and remotely detect radioactive sources in transit, one solution proposed [3] is the deployment of a large network of spatially distributed detectors. Fast and remote radiation detection requires sophisticated equipment which does not come cheap [3]; yet one inexpensive, possibly miniaturized, radiation detector appropriate for such deployment is the Geiger counter.

Geiger counters merely record radiation rays hitting their internal crystal, regardless they come from the source to be detected, or from naturally occurring background radiation. The question thus is whether the aggregate count is due to background alone or the superposition of background and source. This problem can be formulated as a binary hypothesis test—for this case, a fixed-time interval test—that has received considerable attention in the literature [4]. When detecting radioactive material, however, the perceived rate of count reception at each sensor changes with the distance between the sensor and the source, giving rise to a dynamic, time-inhomogeneous stochastic process. As a result, analytic characterization for the error probabilities in this decision problem is not possible. Yet, such analytic expressions are central to constructing optimal, with respect to detection probability, motion control strategies for the mobile sensors.

Work supported in part by ARL MAST CTA # W911NF-08-2-0004.

All authors are with the Department of Mechanical Engineering, University of Delaware, Newark, DE 19716, USA {jxsun,btanner,poulakas}@udel.edu

For the most part, approaches in available literature may be setting too ambitious goals, attempting at identifying not only the nature of the target but also its location solely based on radiation counters [5] [6] [7]. Such approaches essentially face a combination of problems—detection and localization—which is inherently very challenging, both at an analytical and computational level. For static sensors and source, a location estimator can be constructed, and a sequential probability ratio test can be formed [6]. In addition to target state, intensity estimators have also been developed, within a Bayesian framework [5], [7]. Results support the hypothesis that sensor networks can be effective in remotely detecting static radiation sources. When the source is in motion, however, the associated analytic complexity translates to significantly increased computational complexity, and updating posterior probabilities using Bayes rule, becomes problematic even for networks of modest size [7], and under assumptions on the motion of the source being linear and with constant acceleration. Even then, the sensors' integration window closes once the source escapes their effective range.

In contrast, this paper focuses on one of the constituent problems—namely, detection, as it is shown in [8] that mobile sensors focusing on detection has better performance over the static ones used in [5] [6] [7]. Our objective is to reveal what is the best that can be done, under the *assumption* that the emission characteristics and trajectory of the source are known. The rationale behind this divide-and-conquer strategy is that on one hand, given the security application in mind, one probably has an idea of the type of material that is expected to be found. On the other hand, a multitude of other sensing modalities (e.g. cameras [9]) can be used to detect and track a mobile target; one does not need to track motion based solely on Geiger counters. Now we can go after optimal sensor management strategies solely from a detection performance perspective.

We follow a two-stage approach. At the high level, the sensor coordination strategy is decided aiming at maximizing the probability of classifying correctly the target. At the low layer, the strategy is implemented within the limitations imposed by environmental conditions. In the upper layer, the optimal motion strategy is found analytically in the context of Maximum Principle. The intuitive interpretation of the obtained solution is that sensors are managed optimally if they are brought as close to the source, as quickly as possible. Solving the optimal control problem analytically is made possible in part by treating sensor as single integrators. These lessons are transferred to scenarios where the space in which the sensors move while observing the target is cluttered with

978-1-4799-6923-4/15/$31.00 ©2015 IEEE

obstacles, by incorporating a potential-field based motion planning strategy rooted on navigation functions. In this context, the resulting motion planning problem is interesting on its own accord because the potential function is now time-varying, and the goal is to steer the sensors to a *set*, rather than a single point, since approaching too close to a moving and possibly evading target may not be desirable from an operational point of view.

II. Background: Networked Radiation Detection

Imagine that there is a mobile target which could be carrying a radioactive (point) source of activity a. The trajectory of this target is denoted $x_t(t) \in \mathbb{R}^3$. We assume that $\|\dot{x}_t\| \leq V$ for $t \in [0, T]$. In the specific setting considered in this paper, the target is to be classified as benign or radioactive within a time period of T seconds using a collection of k mobile sensors (radiation counters). The motion of the radiation sensors is controllable, and the trajectory of sensor i for $i \in \{1, \ldots, k\}$ is denoted $x_i(t) \in \mathbb{R}^3$. The source activity a is measured in gamma rays emitted per second (cps). In this way, the source activity has the same units as sensor's i cumulative observations up to time $t \in [0, T]$, denoted $N_t(i)$. For a fixed t and i, $N_t(i)$ is a random variable following a Poisson distribution. Each ray incident on sensor i is an event and the instant that the n th such event occurs at sensor i is denoted $\tau_n(i)$.

Such cumulative observations N_t are due not only to the alleged radioactive source, but also due ubiquitous, naturally occurring, background radiation. In this paper, we assume that the source intensity is comparable to background. The background radiation intensity at the location of sensor i is denoted $b_i > 0$ and in this paper will be considered constant. Sensors cannot differentiate between counts due to source and counts due to background. Although background intensity can often be assumed constant, the *perceived* source intensity by sensor i changes with the distance between the source and sensor i. Specifically, the closer the sensor is to the source, the more gamma rays from the source it is likely to detect. If, for the sake of simplicity, sensors are assumed identical having a cross section coefficient χ, then it is generally accepted [7] that the mean count rate ν_i measured by sensor i would follow an inverse square law with respect to the distance between sensor and source. We take this inverse square relationship to be of the form

$$\nu_i \triangleq \frac{\chi a}{2\chi + \|x_i - x_t\|^2} \quad . \tag{1}$$

Thus, when $\|x_i - x_t\| = 0$, the source is touching the surface of the sensor, and the latter measures exactly half of source's emitted rays.

If a single sensor were to make a decision at time T as to whether the target it is observing is radioactive, it would have to choose between two hypotheses:

- $\mathcal{H}_0$: the target is not radioactive and the mean of the Poisson process which $N_T(i)$ follows is b_i, or
- $\mathcal{H}_1$: the target is radioactive, and the mean of the Poisson process which $N_T(i)$ follows is $b_i + \nu_i$.

In the context of this paper, the decision is made by a single processor—possibly one of the sensors—which collects the information and performs a likelihood ratio test [10]. This processor is called the fusion center.

To analyze this decision problem we need the appropriate mathematical setting. For a given i, $N_t(i)$ is a Poisson process, and we could collect all of them in a k-dimensional Poisson process $\boldsymbol{N}_t = \big(N_t(i), \ldots, N_t(k)\big)$—the bold notation marks vectors formed by stacking vectors or scalars associated to all k sensors. If we consider the set of all possible outcomes—occurrences of such events on all sensors—we form a set Ω. Then we consider a measurable space $(\Omega, \mathscr{F})$, where $\mathscr{F}$ is a σ-algebra on Ω.

Now let $(\mathscr{F}_t^{\boldsymbol{N}} : 0 \leq t \leq T)$ be the filtration generated by $\boldsymbol{N}_t$. Thus, $\mathscr{F}_T^{\boldsymbol{N}}$ represents the collective information obtained from all sensors up to time T. Then, the decision between hypothesis $\mathcal{H}_0$ and $\mathcal{H}_1$ on the basis of $\mathscr{F}_T^{\boldsymbol{N}}$ is equivalent to choosing the correct measure on $(\Omega, \mathscr{F}_T^{\boldsymbol{N}})$. For example the choice of the probability measure $\mathbb{P}_0$ yields a probability space $(\Omega, \mathscr{F}_T^{\boldsymbol{N}}, \mathbb{P}_0)$ consistent with hypothesis $\mathcal{H}_0$; similarly, $\mathbb{P}_1$ with $\mathcal{H}_1$. A particular valuation of $\boldsymbol{N}_T$ is assumed to be an outcome $\omega \in \Omega$, and a test for deciding $\mathcal{H}_1$ takes the form of choosing a set $A_1 \in \mathscr{F}_T^{\boldsymbol{N}}$ and checking whether $\omega \in A_1$. A "false alarm" occurs when we find $\omega \in A_1$ while $\mathcal{H}_0$ is in force. The probability for making such an error is therefore $\mathbb{P}_0(A_1)$. Similarly, missing the radioactive target happens when $\omega \in (\Omega \setminus A_1)$ when $\mathcal{H}_1$ is in force, and the probability for such an error is $\mathbb{P}_1(\Omega \setminus A_1)$.

If $\tau_n(i)$ denotes the time instance at which sensor i recorded its n count and $N_T(i)$ is the total number of counts registered by sensor i up to final time T, a Neyman-Pearson likelihood ratio test for the presence of a source can be of the form [10]

$$\prod_{i=1}^{k} \exp\left(-\int_0^T \nu_i(s)\,\mathrm{d}s\right) \prod_{n=1}^{N_T(i)} \left(1 + \frac{\nu_i(\tau_n(i))}{b_i(\tau_n(i))}\right) \geq \gamma \quad , \tag{2}$$

and methods are known [8] for the analytical selection of threshold γ based on target and sensor trajectories. An optimal motion coordination strategy for the sensors could be one that maximizes the probability detection $\mathbb{P}_1(A_1)$ under an upper bound constraint on the probability of false alarm $\mathbb{P}_0(A_1)$. The challenge for such an optimization is that these probabilities are impossible to express analytically for any nontrivial case of interest. Fortunately, tight upper bounds are known and can be used for the selection of the threshold γ in (2) [8]. The approach in this paper, exploits those bounds to formulate an optimal control problem for the motion of the sensors, and solve this problem analytically.

III. Problem Statement

Assume that the position trajectory of sensor i is controlled through input $u_i(t)$ as in

$$\dot{x}_i = u_i \quad . \tag{3}$$

We assume that there are constraints on control actuation in the form $\|u_i\| \leq u_{\max}$ for some constant $u_{\max} > 0$, and we collect all sensor motion control inputs in a stack vector $\boldsymbol{u} = (u_1, \ldots, u_k)$. Recall (1), and note that since x_i is implicitly determined by u_i, and ν_i is a function of x_i, ν_i is a functional operating on u_i; we thus write it $\nu_i(u_i)$, or more generally $\nu_i(\boldsymbol{u})$. Define now the scalar quantity

$$\mu_i(\boldsymbol{u}) \triangleq 1 + \frac{\nu_i(\boldsymbol{u})}{b_i} \quad . \tag{4}$$

For p being a scalar (control) parameter, it can be shown [8] that an upper bound on the probability of miss $\mathbb{P}_1(\Omega \setminus A_1) = 1 - \mathbb{P}_1(A_1)$ for the fusion center of the network of sensors is analytically expressed as

$$J_{\text{PM}}(\boldsymbol{u}, p) \triangleq \sum_{i=1}^{k} \int_0^T [\mu_i(\boldsymbol{u})^p \log \mu_i(\boldsymbol{u}) - \mu_i(\boldsymbol{u}) + 1] b_i \, \mathrm{d}s \quad , \tag{5}$$

while another upper bound on the probability of false alarm can be set at some value $\alpha \in (0, 1)$ by requiring

$$F(\boldsymbol{u}, p) \triangleq \sum_{i=1}^{k} \int_0^T \left[p\mu_i(\boldsymbol{u})^p \log \mu_i(\boldsymbol{u}) - \mu_i(\boldsymbol{u})^p + 1\right] b_i \, \mathrm{d}s = -\log \alpha \quad . \tag{6}$$

It is therefore natural to formulate an optimal control problem, where J_{PM} is a cost to be optimized with respect to $\boldsymbol{u}$ and p under constraint (6). In this problem, the state of the dynamical system is $\boldsymbol{\mu} \triangleq (\mu_1, \ldots, \mu_k)$, implicitly determined by $\boldsymbol{u}$ in (4) via (1) and (3); specifically,

$$\dot{\mu}_i = \frac{2\chi a(x_t - x_i)}{b_i(2\chi + \|x_t - x_i\|^2)^2}(u_i - \dot{x}_t) \quad . \tag{7}$$

IV. Optimal Sensor Management: Analytic Solutions

The path to an analytic solution starts with transforming the constrained optimal control problem (5)–(6) into an unconstrained one. The first partial result establishes the monotonicity of functional F in (6) with respect to the positive parameter p.

Lemma 1: For fixed $\boldsymbol{u}$, F is strictly increasing with p.

Proof: Write $\frac{\partial F}{\partial p} = \sum_{i=1}^{k} \int_0^T p \, \mu_i^p \, (\log \mu_i)^2 \, \mathrm{d}t$, and note that it is strictly positive since $\mu_i > 1$. ■

The next step is to establish the existence of a function from $\boldsymbol{\mu}$ to p.

Lemma 2: The (functional) mapping $\boldsymbol{\mu} \mapsto p$, denoted ϕ, associates to each $\boldsymbol{\mu}$ a unique p.

Proof: It follows from Lemma 1 and the Implicit Function Theorem. ■

We henceforth write

$$p = \phi(\boldsymbol{\mu}) \quad . \tag{8}$$

Lemma 3: For all $t_1 \in (0, T]$, it is $\left.\frac{\delta \phi(\boldsymbol{\mu})}{\delta \mu_i}\right|_{t_1} \leq 0$.

Proof: Consider first a needle perturbation of the form $\epsilon\delta(t - t_1)$ on coordinate i of $\boldsymbol{\mu}$, yielding a perturbed $\tilde{\boldsymbol{\mu}}$ with component $\mu_i(t) + \epsilon\delta(t - t_1)$; here, $\delta(t - t_1)$ is the Dirac function offset at t_1 and $\epsilon > 0$ a small parameter. Using Taylor expansion on the integrand of $F(\boldsymbol{\mu}, p)$ we find

$$F(\tilde{\boldsymbol{\mu}}, p) \approx F(\boldsymbol{\mu}, p) + b_i \epsilon p^2 \mu_i(t_1)^{p-1} \log \mu_i(t_1) \quad ,$$

from which the first order variation in $F(\boldsymbol{\mu}, p)$ due to $\epsilon\delta(t - t_1)$ in μ_i is obtained

$$F(\tilde{\boldsymbol{\mu}}, p + \delta p) - F(\boldsymbol{\mu}, p) = b_i \epsilon p^2 \mu_i(t_1)^{p-1} \log \mu_i(t_1) + \frac{\partial F}{\partial p} \delta p,$$

which is zero because F is constrained to $-\log \alpha$:

$$\delta p = -\frac{\epsilon \; b_i p^2 \; \mu_i^{p-1} \log \mu_i \Big|_{t_1}}{\sum_{i=1}^{k} \int_0^T p \, \mu_i^p \; \log^2 \mu_i \, \mathrm{d}t}. \quad (Given\ Lemma\ 1)$$

Rewriting $p = \phi(\boldsymbol{\mu})$, it follows

$$\left.\frac{\delta \phi(\boldsymbol{\mu})}{\delta \mu_i}\right|_{t_1} = \lim_{\epsilon \to 0} \frac{\delta p}{\epsilon} < 0$$

and the proof is completed. ■

We are now ready to apply the Maximum Principle and extract the optimal motion coordination strategy for each sensor.

Proposition 1: The solution for sensor $i \in \{1, \ldots, k\}$ to the optimal control problem (5)–(7) within the feasible set $\mathcal{U} = \{\boldsymbol{u} \in \mathbb{R}^{3k} : \|u_i\| \leq u_{\max}\}$, is

$$u_i = \begin{cases} \frac{x_t - x_i}{\|x_t - x_i\|} u_{\max} & \text{if } x_i \neq x_t \\ \dot{x}_t & \text{if } x_i = x_t \end{cases}$$

Proof: Given (8), the cost functional is written

$$J_{\text{PM}} = \sum_{i=1}^{k} \int_0^T (\mu_i^{\phi(\boldsymbol{\mu})} \log \mu_i - \mu_i + 1) b_i \, \mathrm{d}t$$

Since J_{PM} is always finite, by Fubini's theorem,

$$J_{\text{PM}} = \int_0^T \sum_{i=1}^{k} (\mu_i^{\phi(\boldsymbol{\mu})} \log \mu_i - \mu_i + 1) b_i \, \mathrm{d}t \quad .$$

The Hamiltonian is

$$H = \sum_{i=1}^{k} \lambda_i \dot{\mu}_i(u_i) - \sum_{i=1}^{k} (\mu_i^{\phi(\boldsymbol{\mu})} \log \mu_i - \mu_i + 1) b_i \quad , \tag{9}$$

and dynamics of costates λ_i is written

$$\dot{\lambda}_i = -\frac{\partial H}{\partial \mu_i} = \left(\phi(\boldsymbol{\mu}) \mu_i^{\phi(\boldsymbol{\mu})-1} \frac{\delta \phi(\boldsymbol{\mu})}{\delta \mu_i} \log \mu_i + \mu_i^{\phi(\boldsymbol{\mu})-1} - 1\right) b_i$$

Since $\mu_i > 1$ and $\phi(\boldsymbol{\mu}) \in (0, 1)$, we have $0 < \mu_i^{\phi(\mu)-1} < 1$, and therefore

$$\dot{\lambda}_i < b_i \mu_i^{\phi(\boldsymbol{\mu})-1} \phi(\boldsymbol{\mu}) \frac{\delta \phi(\boldsymbol{\mu})}{\delta \mu_i} \log \mu_i \overset{\text{Lemma 3}}{\leq} 0 \tag{10}$$

for all $t \in (0, T]$.

Now, since $\mu_i^*(T)$ is free in $(1, 1 + \frac{a}{2b}]$, we have two scenarios: $\mu_i^*(T) \in (1, 1 + \frac{a}{2b})$ or $\mu_i^*(T) = \mu_{i_{max}} = 1 + \frac{a}{2b}$. If $\mu_i^*(T) \in (1, 1 + \frac{a}{2b})$, the transversality condition requires $\lambda_i(T) = 0$. Thus, given (10), it is $\lambda_i(t) > 0 \;\; \forall t \in (0, T]$. In light of this, and given (7), the Hamiltonian maximization condition $H(\boldsymbol{\mu}^*, \boldsymbol{u}^*, \boldsymbol{\lambda}^*) = \max_{\boldsymbol{u} \in \mathcal{U}} H(\boldsymbol{\mu}^*, \boldsymbol{u}^*, \boldsymbol{\lambda}^*)$ applied on (9) requires that

$$u_i^* = \frac{x_t - x_i}{\|x_t - x_i\|} u_{\max} \quad , \tag{11}$$

that is, to employ the maximal control effort to close the distance between sensor and source. Using such controller, $\mu_i^*(T) = \mu_{i_{max}}$ eventually given enough time T, which takes us to the second type end condition, let such switching time be T_s. Now we consider the system in $[T_s, T]$ with boundary condition $\mu_i(T_s) = \mu_i(T) = \mu_{i_{max}}$, notice the fact that $\frac{\delta J_{PM}}{\delta \mu_i} = \lambda_i < 0$. To minimize J_{PM} when $t \in [T_s, T]$, we want to keep μ_i at its maximum value and $u_i = \dot{x}_t$. ■

Essentially what Proposition 1 dictates is for the sensor platforms to close the gap between themselves and the suspected target as fast as possible and remain close.

V. Extension to constrained environments

Limiting the feasible positions that sensors can attain augments the set of constraints in the optimal control problem formulation (5)–(6). In the general case, the resulting optimal control problem may not admit analytic solutions any more. Even if such solutions can be found, it is conceivable that the optimal controls steer the sensors right at the boundary of the feasible state set, at an effort to increase the lower bound on the detection probability to the maximum degree possible. Practically, this control action would lead the mobile sensor platforms to graze obstacle boundaries. These considerations motivate an alternative, suboptimal approach to sensor management, which—while adhering to the same principle of closing the distance as quickly as possible—is likely to trade-off some performance for safety and the ability to still analytically establish convergence properties for the closed loop system.

Using the insight obtained from the unconstrained case, we develop a sensor management strategy for navigation amongst obstacles in the context of navigation functions. Instead of running at full speed toward the target, sensors are now supposed to perform steepest descent over a smooth artificial landscape in which obstacles are regions of high elevation and the target sits around an area of depression. The latter attribute of this landscape is motivated from the fact that we cannot allow the sensor platforms to physically touch and collide with their target, but rather keep them at a minimum safe distance r_t away from it. The destination for the sensors thus becomes a *set*, the surface of a sphere centered at the moving target. Another technical challenge is that this destination set is time-varying. Inevitably, the convergence problem becomes one where the underlying system is time-varying—fully knowing the target's trajectory is not sufficient to reduce the system into a time-invariant one, because the obstacles can be fixed.

For sensor i at position x_i, the goal function that the potential field attempts to minimize takes the form

$$J_i(x_i, t) = (\|x_i - x_t(t)\|^2 - r_t^2)^2 \ .$$

It can be shown that J has two distinct sets of critical points, one isolated point at x_r which is a local maximum, and a manifold of local minima on the boundary of the sphere $B_{r_t}(x_t)$ defined by $\|x_i - x_t(t)\|^2 - r_t^2 = 0$.

Since so far we have treated the sensors as point masses (negligible volume) we will ignore the possibility of them colliding with each other and focus on steering them away from environment obstacles. In the spirit of the preliminary sphere-world analysis of [11], these obstacles are assumed to be spherical, which can be extended to star shape [12]. The boundary of obstacle $j \in \{0, \ldots, m\}$, having radius ρ_j and center o_j is described by means of the function $\beta_{i\,j} = \|x_i - o_j\|^2 - \rho_j^2$,which vanishes on the obstacle's boundary and is positive in the space surrounding it. Index 0 marks the outer workspace boundary, of radius ρ_0, this one expressed in the form $\beta_{i\,0} = \rho_0^2 - \|x_i\|^2$.With obstacles being isolated, static, and at least r_t away from the target $\forall\, t \in [0, T]$—these three requirements correspond to the collision-free workspace remaining *valid* [11], at least during the sensors' integration window—the following construction gives rise to a single scalar function that serves as a metric of proximity to (any) obstacle boundary, $\beta_i = \prod_{j=0}^{M} \beta_{i\,j}$.

The following statement can be proved, but the proof itself is nontrivial and too lengthy for the space constraints of this paper. Deferring its presentation to a subsequent paper, we refrain from stating the claim as a theorem and instead call it a conjecture:

Conjecture 1: Given that the space is valid, there exists a positive integer N such that for every $k \geq N$, the function

$$\varphi_i(x_i, x_t) = \frac{J_i(x_i, x_t)}{\left(J_i(x_i, x_t)^k + \beta_i(x_i)\right)^{1/k}} \quad (12)$$

is such that all critical points other than those in $\partial B_{r_t}(x_t)$ are either nondegenerate with attraction regions of measure zero or in $\mathring{B}_{r_t}(x_t)$, and the gradient field generated by $\nabla_{x_i}\varphi_i$ has $\partial B_{r_t}(x_t)$ as the only limit set with non-zero measure attraction region outside $\mathring{B}_{r_t}(x_t)$.

And we require that $x_i(0) \notin \mathring{B}_{r_t}(x_t(0))$. Thus Proposition 2 guarantees that $x_i(t) \notin \mathring{B}_{r_t}(x_t(t))$ due to $\dot{\varphi} \leq 0$.

There are some practical considerations related with the application of a bang-bang controller like (11) within a constrained environment, especially when it is undesirable for sensor platforms to collide with their target at maximum speed. Even when the system's manifold of attractors is set at a safe distance r_t away from the target, flowing along the direction of the negated gradient of (12) at full speed is certain to result to overshoot and oscillatory behavior in the neighborhood of the attracting set. The sensors' approach to this goal set needs to be fast but gradual. For these reasons, and assuming the truth of Conjecture 1, a relaxation on (11) for implementation in constrained environments can take the form

$$u_i^\circ = -c\frac{\nabla_{x_i}\varphi_i}{\|\nabla_{x_i}\varphi_i\| + \xi} - (\nabla_{x_t}\varphi_i^\intercal\, \dot{x}_t)\frac{\nabla_{x_i}\varphi_i}{\|\nabla_{x_i}\varphi_i\|^2} \ , \quad (13)$$

for some constants $c < u_{\max}$, and $\xi > 0$.

Control law (13) is essentially a modulated (negated) gradient following tracking controller with a feedforward to compensate for target motion. It can be shown that assuming that $\sup_{t\geq 0}\|\dot{x}_t(t)\|$ is sufficiently smaller compared to $u_{\max}$, then (c, ξ, ϵ) can be always be chosen so that both (a) $\|u_i^\circ\| \leq u_{\max}$ for all $\cap_{j=0}^{m}\{x_i | \beta_{ij}(x_i) \geq \epsilon\}$, and (b) (gradual) convergence to the surface of the ball of radius r_t around the target is analytically established.The former claim, on the boundedness of (13), relates to lower bounding $\|\nabla_{x_i}\varphi_i\|$ which appears in the denominator of the second term. This term vanishes as x_i approaches one of the critical points of φ_i. For a properly tuned navigation function, those critical points can be expected to be in a set $\cup_{j=0}^{m}\{x_i|\beta_{ij}(x_i)<\epsilon\}\cup\partial B_{r_t}(x_t)\cup\mathring{B}_{r_t}(x_t)$; we shall prove that provided that along the sensor trajectory it always satisfies $\cap_{j=0}^{m}\{x_i|\beta_{ij}(x_i)\geq\epsilon\}$, the magnitude of the control input is upper bounded. We need to note, however, that $\beta_{ij}(x_i)\geq\epsilon$ cannot be guaranteed a priori for all initial conditions; there will be a set of initial conditions around the attraction regions of the unstable critical points of φ_i that generate trajectories which cross into $\cup_{j=0}^{m}\{x_i|\beta_{ij}(x_i)<\epsilon\}$. Thus in principle, one can compute $\underline{\varphi_i}\triangleq\inf_{x_i:\cup_{j=0}^{m}\{x_i|\beta_{ij}(x_i)<\epsilon\}}\varphi_i$, and consider only initial conditions that satisfy $\varphi_i\big(x_i(0)\big)<\underline{\varphi_i}$.

Assuming from now on that $\beta(x_i)\geq\epsilon$, we set on to see why u_i° can be bounded. First need to state a few lemmas, the proofs of which are abbreviated due to space limitations.

Lemma 4: If $\forall j,\beta_{ij}(x_i)\geq\epsilon>0$, then $\|\frac{\nabla_{x_i}\beta_i}{\beta_i}\|$ admits an upper bound.

Proof: (sketch) One shows that over $\cap_{j=0}^{m}\{x_i|\beta_{ij}(x_i)\geq\epsilon\}$, $\sup\|\frac{\nabla_{x_i}\beta_i}{\beta_i}\|\leq\frac{2}{\epsilon}\sum_{j=0}^{M}\sup\|x_i-o_j\|$. ■

Lemma 5: If $\forall j,\beta_{ij}(x_i)\geq\epsilon>0$, then $\|\frac{\nabla_{x_i}J_i}{J_i}\|$ admits a a positive lower bound.

Proof: (sketch) We know that $\|x_i-x_t\|\geq r_t$ according to Proposition 2. One shows that over $\{x_i|\|x_i-x_t\|\geq r_t\}$, $\inf\frac{\|\nabla_{x_i}J_i\|}{J_i}>\frac{4r_t}{\sup\{\|x_i-x_t\|^2-r_t^2\}}>0$. ■

Lemma 6: If $\forall j,\beta_{ij}(x_i)\geq\epsilon>0$, then $k\|\frac{\nabla_{x_i}J_i}{J_i}\|-\|\frac{\nabla_{x_i}\beta_i}{\beta_i}\|\geq\delta$.

Proof: (sketch) It is straightforward to show that it suffices to pick $k\geq\delta\inf\big\{\frac{\|\nabla_{x_i}J_i\|}{J_i}\big\}^{-1}+\frac{\sup\big\{\|\frac{\nabla_{x_i}\beta_i}{\beta_i}\|\big\}}{\inf\big\{\frac{\|\nabla_{x_i}J_i\|}{J_i}\big\}}$. Lemmas 4 through 5 ensure that the right hand side is upper bounded, and therefore an appropriately large parameter k can be selected to establish δ as a lower bound. ■

Now we are in position to show that u_i° is bounded.

Lemma 7: If $\forall j,\beta_{ij}(x_i)\geq\epsilon>0$, then u_i° is bounded.

Proof: (sketch) First show that $\|u_i^\circ\|<c+k\|\frac{\nabla_{x_i}J_i}{J_i}\|\cdot\big(\|k\frac{\nabla_{x_i}J_i}{J_i}-\frac{\nabla_{x_i}\beta_i}{\beta_i}\|\big)^{-1}\|\dot{x}_t\|$, and then confirm that for a big enough k, the inequality can be strengthened into

$$\|u_i^\circ\|<c+\|\dot{x}_t\|+\frac{\|\frac{\nabla_{x_i}\beta_i}{\beta_i}\|}{k\|\frac{\nabla_{x_i}J_i}{J_i}\|-\|\frac{\nabla_{x_i}\beta_i}{\beta_i}\|}\|\dot{x}_t\|\ .$$

Boundedness now follows from Lemmas 4 through 6. ■

Proposition 2: The closed loop system (3)–(13) converges to the set $\{x_i\in\mathbb{R}^3:J_i(x_i,x_t)=0\}$, from almost everywhere in $\{x_i\in\mathbb{R}^3:\beta_i(x_i)>0,x_i\notin\mathring{B}_{r_t}(x_t)\}$.

Proof: The closed loop system is time-varying due to $x_t(t)$. The proof is thus based on Barbalat's lemma using function φ_i. The aim is to show that $\lim_{t\to\infty}\dot{\varphi}_i=0$.

First note that $\varphi_i\geq0$. Then expand $\dot{\varphi}_i$ and plug (13) to verify that

$$\dot{\varphi}_i=-c\frac{\|\nabla_{x_i}\varphi_i\|^2}{\|\nabla_{x_i}\varphi_i\|+\xi}\leq0\ . \qquad (14)$$

So $\lim_{t\to\infty}\varphi_i$ exists and bounded. Thus according to Barbalat's lemma, proving that $\lim_{t\to\infty}\dot{\varphi}_i=0$ reduces to showing that $\dot{\varphi}_i$ is uniformly continuous in t, which can be ensured if $\ddot{\varphi}_i$ is bounded. Toward this end note that

$$\ddot{\varphi}=-c\frac{1-\frac{1}{2}\|\nabla_{x_i}\varphi_i\|}{(\|\nabla_{x_i}\varphi_i\|^2+\xi)^2}\frac{\mathrm{d}\|\nabla_{x_i}\varphi_i\|^2}{\mathrm{d}t}\ ,$$

and is bounded if $\frac{\mathrm{d}\|\nabla_{x_i}\varphi_i\|^2}{\mathrm{d}t}$ is. Indeed,

$$\begin{aligned}\tfrac{\mathrm{d}\|\nabla_{x_i}\varphi_i\|^2}{\mathrm{d}t}&=-2\frac{\nabla_{x_i}\varphi_i^\intercal\,[\nabla_{x_i}^2\varphi_i]\,\nabla_{x_i}\varphi_i}{\|\nabla_{x_i}\varphi_i\|+\xi}\\&\quad-2\frac{\nabla_{x_t}\varphi_i^\intercal\dot{x}_t}{\|\nabla_{x_i}\varphi_i\|^2}\nabla_{x_i}\varphi_i^\intercal[\nabla_{x_i}^2\varphi_i]\nabla_{x_i}\varphi_i\\&\quad+2\nabla_{x_i}\varphi^\intercal[\nabla_{x_i}(\nabla_{x_t}\varphi_i)]\dot{x}_t\ .\end{aligned}$$

With φ_i being a smooth function, its first and second partial derivatives are bounded on the compact subset of $\mathbb{R}^3$ where $\beta_i\geq0$. The denominator of the second term does not raise a problem because $\big|\frac{\nabla_{x_i}\varphi_i^\intercal\,[\nabla_{x_i}^2\varphi_i]\,\nabla_{x_i}\varphi_i}{\|\nabla_{x_i}\varphi_i\|^2}\big|$ admits an upper bound equal to the maximum eigenvalue of the Hessian of φ_i—which is finite. Therefore, since $\|\dot{x}_t\|<V$, $\frac{\mathrm{d}\|\nabla_{x_i}\varphi_i\|^2}{\mathrm{d}t}$ is bounded, $\dot{\varphi}_i$ is uniformly continuous, and by Barbalat it follows that $\lim_{t\to\infty}\dot{\varphi}_i=0$. Then (14) implies that $\lim_{t\to\infty}\|\nabla_{x_i}\varphi_i\|=0$, which in turns suggests—based on Conjecture 1—that with time $x_i\to\{x\in\mathbb{R}^3:J_i(x,x_t)=0\}$ from almost all initial conditions in $\{x_i\in\mathbb{R}^3:\beta_i(x_i)>0,x_i\notin\mathring{B}_{r_t}(x_t)\}$. ■

VI. Simulations

A $2\,\frac{1}{2}$ dimensional space simulation scenario (the environment geometry is invariant along the third spatial coordinate) is used to test the control law. Its two-dimensional projection is depicted in Fig. 1. Sensor and source physical volumes are neglected. The target is following a sinusoid trajectory starting initially at point $(x,y)=(15,0)$(m). Its x velocity is constantly 0.3π(m/s) and y velocity is given as $0.3\pi\cos(\frac{\pi}{50}t)$(m/s). It is assumed that the target's position and velocity is known to all sensors.

Applying control law (13) to each sensor dynamics (3), results in the motion behavior shown in Fig. 1. By closing the distance between themselves and the target while navigating their cluttered workspace, they increase their signal-to-noise ratio of their radiation measurements. We consider a sensor (time) integration window $T=130$ s, after which sensors are called to make a decision based on their measurements as to whether the target they were tracking was radioactive.

The target is indeed radioactive, with an activity of $a=2.4\times10^6$ (Poisson mean) counts per minute, while the background radiation is taken to be at a level of $b=10$ counts per minute. Despite this large difference, the sensor geometric characteristics as expressed by the cross-section coefficient $\chi=10^{-4}m^2$ combined with the inverse square distance effect render the average *perceived* source activity ν_i (see (1)) at the sensor's location comparable to background.

Along these paths, we record 2 sample sets of 73 778 i.i.d. two-minute histories of simulated radiation measurements.

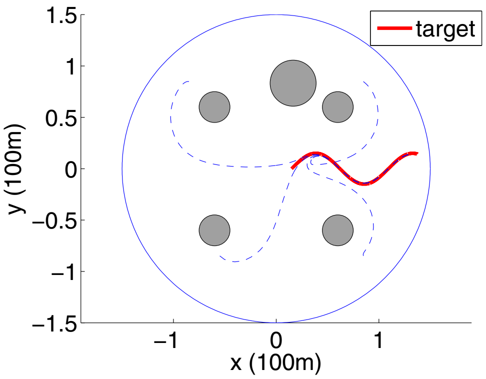

Fig. 1: A 2D simulation scenario. A source carrying target is circling the origin and its path is shown as a thick (red) curve. Four mobile sensors start moving from initial positions behind disk-shaped obstacles, and navigate along the dashed-line paths toward the source's neighborhood following the gradient field of a time-varying navigation function. Sensors collect measurements for a time window of two minutes before they make a decision as to whether the target is radioactive.

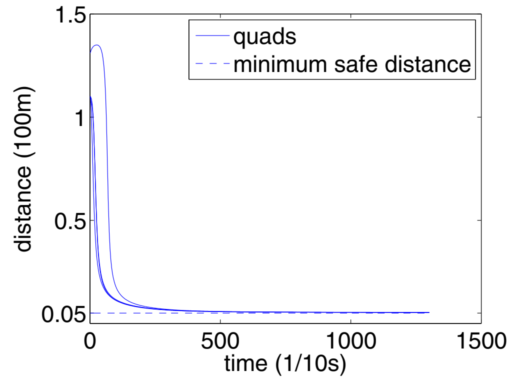

Fig. 2: Distance between sensors and target. Our simulation testbed refers to mobile sensors as quads, envisioning quadrotors equipped with Geiger counters.

The target is set to be radioactive in one set and benign in the other. For each sample, we perform a binary hypothesis test (2) with a threshold of $\gamma = 3.4$, designed to guarantee a false alarm rate of less than $1\,\%$ [8]. Monte Carlo methods empirically estimate the probability of false alarms and correct detection at an accuracy level of $\varepsilon = 0.005$ and confidence of $95\,\%$ [13]. These estimates are $0.12\,\%$ for the false alarm, and $99.42\,\%$ for the detection rate.

VII. Conclusion

Under certain simplifying assumptions, sensor mobility can be optimally utilized in the context of networks of radiation counters to boost detection performance in low-rate radiation activity detection scenarios. In the problem at hand, the suspected source is mobile, and sensors have knowledge of its position and velocity. Analytic optimal control solutions point to motion coordination strategies that tend to minimize the distance between sensor and suspected source as quickly as possible, resembling bang-bang minimum-time solutions to optimal control problems. Taking this lesson from the analytical, closed-form solutions obtained for sensor motion in unconstrained environments, we develop motion planning strategies for sensor coordination and navigation in obstacle environments with bounds on actuation effort. The motion planning methodology is based on gradient descent along potential fields generated by a special type of time-varying navigation functions. The resulting control laws are feedback-based and reactive to the source's motion, ensuring asymptotic tracking of the mobile source in addition to obstacle avoidance. The control strategy is tested in simulation on a two-dimensional detection scenario, and the detection efficiency is confirmed through Monte Carlo analysis.

References

[1] R. C. Archibold and R. Gladstone, "Truck With Lethal Load Is Recovered in Mexico," The New York Times, pp. A12, Dec. 5 2013.

[2] W. J. Broad, "The Nun Who Broke Into the Nuclear Sanctum," The New York Times, pp. A1, Aug. 11 2012.

[3] R. Byrd, J. Moss, W. Priedhorsky, C. Pura, G. Richter, K. Saeger, W. Scarlett, S. Scott, and R. Wagner, Jr., "Nuclear detection to prevent or defeat clandestine nuclear attack," *IEEE Sensors Journal*, vol. 5, no. 4, pp. 593–609, 2005.

[4] P. Brémaud, *Point Processes and Queues*. Springer-Verlag, 1981.

[5] S. Brennan, A. Mielke, and D. Torney, "Radioactive source detection by sensor networks," *IEEE Transactions on Nuclear Science*, vol. 52, no. 3, pp. 813–819, 2005.

[6] J.-C. Chin, N. S. V. Rao, D. K. Y. Yau, M. Shankar, Y. Yang, J. C. Hou, S. Srivathsan, and S. Iyengar, "Identification of low-level point radioactive sources using a sensor network," *The ACM Transactions on Sensor Networks*, vol. 7, no. 3, pp. 21:1–21:35, 2010.

[7] R. Nemzek, J. Dreicer, D. Torney, and T. Warnock, "Distributed sensor networks for detection of mobile radioactive sources," *IEEE Transactions on Nuclear Science*, vol. 51, no. 4, pp. 1693–1700, 2004.

[8] C. D. Pahlajani, J. Sun, I. Poulakakis, and H. G. Tanner, "Error probability bounds for nuclear detection: Improving accuracy through controlled mobility," *Automatica*, vol. 50, no. 10, pp. 2470 – 2481, 2014.

[9] H. Wei, W. Lu, P. Zhu, G. Huang, J. Leonard, and S. Ferrari, "Visibility-based motion planning for active target tracking and localization," in *Proceedings of the IEEE/RSJ International Conference on Intelligent Robots and Systems*, Chicago, Illinois, Sept. 2014, pp. 76–82.

[10] C. D. Pahlajani, I. Poulakakis, and H. G. Tanner, "Networked decision making for poisson processes with applications to nuclear detection," *IEEE Transactions on Automatic Control*, vol. 59, no. 1, pp. 193–198, 2014.

[11] D. E. Koditschek and E. Rimon, "Robot navigation functions on manifolds with boundary," *Advances in Applied Mathematics*, vol. 11, no. 4, pp. 412–442, 1990.

[12] E. Rimon and D. Koditschek, "The construction of analytic diffeomorphisms for exact robot navigation on star worlds," in *IEEE International Conference on Robotics and Automation*, Scottsdale, Arizona, May 1989, pp. 21–26 vol.1.

[13] M. Vidyasagar, "Statistical learning theory and randomized algorithms for control," *IEEE Control Systems Magazine*, vol. 18, no. 6, pp. 69–85, 1998.